


# Preparation and Evaluation of Chitosan Coated PLGA Nanoparticles Encapsulating Ivosidenib with Enhanced Cytotoxicity Against Human Liver Cancer Cells

Bader B Alsulays , Alhussain H Aodah, Mohammad Muqtader Ahmed, Md Khalid Anwer

Department of Pharmaceutics, College of Pharmacy, Prince Sattam Bin Abdulaziz University, Al-Kharj, 11942, Saudi Arabia

Correspondence: Bader B Alsulays, Department of Pharmaceutics, College of Pharmacy, Prince Sattam Bin Abdulaziz University, P.O. Box 173, Al-Kharj, Saudi Arabia, Tel +966-554112830, Email b.alsulays@psau.edu.sa

**Purpose:** Ivosidenib (IVO), an isocitrate dehydrogenase-1 (IDH1) used for treatment of acute myeloid leukemia (AML) and cholangiocarcinoma. However, poor solubility, low bioavailability, high dose and side effects limit clinical application of IVO.

**Methods:** Ivosidenib-loaded PLGA nanoparticles (IVO-PLGA-NPs) and Ivosidenib-loaded chitosan coated PLGA nanoparticles (IVO-CS-PLGA-NPs) were prepared using emulsification and solvent evaporation method for the treatment of liver cancer.

**Results:** The developed IVO-PLGA-NPs were evaluated for their particle size ( $171.7 \pm 4.9$  nm), PDI (0.333), ZP ( $-23.0 \pm 5.8$  mV), EE ( $96.3 \pm 4.3\%$ ), and DL ( $9.66 \pm 1.1\%$ ); similarly, the IVO-CS-PLGA-NPs were evaluated for their particle size ( $177.3 \pm 5.2$  nm), PDI (0.311), ZP  $+25.9 \pm 5.7$  mV, EE ( $90.8 \pm 5.7\%$ ), and DL ( $9.42 \pm 0.7\%$ ). The chitosan coating of IVO-PLGA-NPs was evidenced by an increase in mean particle size and positive ZP value. Because of the chitosan coating, the IVO-CS-PLGA-NPs showed a more stable and prolonged release of IVO than IVO-PLGA-NPs. In comparison to pure-IVO, the IVO-PLGA-NPs and IVO-CS-PLGA-NPs were found to be more effective against HepG2 cells, with  $IC_{50}$  values for the MTT assay being approximately half of those of pure-IVO. In HepG2 cells, the expressions of caspase-3, caspase-9, and p53 were significantly ( $p < 0.05$ ) elevated.

**Conclusion:** Overall, these findings suggest that chitosan coating of IVO-PLGA-NPs improves the delivery and efficacy of ivosidenib in liver cancer treatment.

**Keywords:** polymers, characterization, bioavailability, sustained release, caspase

## Introduction

Liver cancer is one of the most common cancers globally, and one of the highest cause of the cancers related death. Most of the liver cancer cases were in the form of Hepatocellular carcinoma (HCC). Lack of effective treatment is the main reason of high mortality rate. The classical chemotherapy is insufficient and there is a significant chemoresistance of HCCs.<sup>1-3</sup> Ivosidenib, is a newly FDA approved drug for the treatment of adults with relapsed or refractory acute myeloid leukemia. It is an inhibitor of mutated cytosolic isocitrate dehydrogenase 1 (IDH1). Cholangiocarcinoma, solid tumor and other tumors are other indications of Ivosidenib, which are now undergoing clinical development worldwide.<sup>4-6</sup> It is classified as BCS class II drug with poor solubility and high permeability.<sup>7</sup> The poor aqueous solubility will further affect the bioavailability of the drug and limit its clinical effect. In order to improve the solubility of poorly soluble drug, many techniques, such as solid dispersion, salt formation, complexation, and nanoparticle were employed. Among these techniques, nanoparticle has gained considerable attention and extensively investigated in the pharmaceutical industry. Due to its advantages in improving drug solubility, bioavailability, stability and high encapsulation efficiency, polymeric nanoparticles were frequently used in drug development.<sup>8,9</sup> Nanostructures offer a promising solution to the challenges faced in the treatment of liver cancer, particularly in combating drug resistance. The ability of nanostructures to deliver

drugs directly to cancer cells can help overcome issues such as limited drug penetration and efficacy, as well as reduce systemic toxicity.<sup>10</sup>

Biodegradable polymers which used in polymeric nanoparticle formulation have some benefits of being less toxic and its role in improving the physiochemical properties of poorly soluble drugs. PLGA, short for poly(lactic-co-glycolic acid), is a remarkable polymer that has gained considerable recognition in the realm of biomedical research and pharmaceutical development. It is US-FDA approved copolymer, making it a highly trusted choice for the preparation of various polymeric nanoparticle-based formulations. Many applications of this polymer including enhancing the solubility, bioavailability, and stability have been reported. PLGA polymers play a crucial role in delivering anticancer drugs directly to tumor sites, maximizing treatment efficacy while minimizing side effects. The ability of PLGA to encapsulate and release drugs in a controlled manner enhances the therapeutic outcomes of cancer treatments.<sup>11,12</sup> Although, many advantages of PLGA NPs, it impart negative surface potential, which decrease the mucoadhesive properties as well as the bioavailability.<sup>13–15</sup>

In order to overcome this problem, surface modification of PLGA NP using different polymers was beneficial. Chitosan is one of the biodegradable polymer with good mucoadhesive properties, can be used for this purpose. Due to its positive surface charge, coating the PLGA NP with chitosan can enhance the cellular absorption and mucoadhesion.<sup>8</sup> Chitosan coating holds great potential in optimizing nanoparticle-based drug delivery systems. Its unique properties offer improved stability, controlled release mechanisms and targeted delivery capabilities.<sup>16–18</sup> Chitosan nanoparticles have shown great potential in improving the bioavailability and targeted delivery of anti-cancer drugs. Their small size and biocompatibility allow for efficient penetration into tumor tissues while minimizing systemic toxicity.<sup>19–21</sup> The current work is novel because it is the first to be cited in the literature on the repurposing of ivosidenib and its developed polymeric nanoparticles for enhanced anticancer activity against liver cancer cells. This is a novel idea that needs more investigation since it has great potential to treat liver cancer, which is driving up healthcare expenditures worldwide.

In this study, we prepared IVO-PLGA-NP and IVO-CS-PLGA-NP by emulsification and solvent evaporation technique using an ultrasonic probe. The developed formulations were assessed in terms of drug encapsulation, ZP, PDI, and particle size. The DSC and FTIR studies were carried out to check compatibility between drugs and polymers. Studies on drug release in vitro, storage stability, and in vitro cytotoxicity were conducted on HepG2 cells.

## Materials and Methods

### Materials

Ivosidenib (IVO) was procured from “Beijing Mesochem Technology Co. Ltd (Beijing China)”. Poly (lactic-co-glycolic acid) (PLGA, 50:50), kolliphor-188, dichloromethane (DCM), and methanol were bought from “Sigma-Aldrich (St. Louis, USA)”. The Merck MilliQ Millipore ultrapure water purification system was used to prepare MilliQ water on-site. “Dulbecco’s Modified Eagle Medium (DMEM)” was bought from “Life Technologies Ltd. (Paisley, UK)”.

### Preparation of IVO-PLGA-NPs and IVO-CS-PLGA-NPs

The process of emulsification and solvent evaporation was utilized to prepare NPs loaded with IVO.<sup>22</sup> Briefly, PLGA (25 mg/mL) polymeric solution in dichloromethane was prepared, and IVO (10 mg) was dissolved in it to obtain the organic phase. Conversely, a separate aqueous phase containing 1% w/v of kolliphor-188 was prepared (Table 1), then under probe sonication “(Fisher scientific; United States)” for 6 minutes at 65% W voltage efficiency for 5 minutes, the aqueous phase was added to the organic phase using a syringe at a rate of 0.5 mL/min to emulsify it. The organic solvent

**Table 1** Formulation Composition of IVO-PLGA-NPs and IVO-CS-PLGA-NPs

Formulations	IVO (mg)	PLGA (mg)	Chitosan (mg)	P-188 (%w/v)
Blank PLGA-NPs	-	50	-	1
IVO-PLGA-NPs	10	50	-	1
IVO-CS-PLGA-NPs	10	50	50	1

was evaporated under magnetic stirrer for 4 hours. The nanoparticles (IVO-PLGA-NPs) were collected after centrifugation at 16,000 rpm for 10 minutes. The obtained sediment was washed three times with distilled water, then lyophilized (Millrock Technology, Kingston, NY, USA). The chitosan-coated PLGA-NPs was prepared by addition of previously prepared IVO-PLGA-NPs in chitosan solution (0.5% w/v in glacial acetic acid) with continuous stirring at 400 rpm for 12 hours.

## Measurement of Mean Particle Size, Polydispersity Index (PDI), and Zeta Potential

The IVO-PLGA-NPs, IVO-CS-PLGA NPs, and blank-PLGA NPs were measured for particle size and PDI using “Zetasizer™ NanoZS (Malvern Instrument Ltd., Malvern, UK)” instrument. The nanoparticles were dispersed in deionized water as dispersion medium prior to analysis, and equilibrated for 3 min at 25 °C. The measurements were carried out at a 173° detection angle using a non-invasive backscatter technique.<sup>23</sup> Every measurement was performed in triplicate, and the mean and standard deviation were noted. The software’s built-in Smoluchowski approximation was used to calculate the nanoparticles zeta potential, which allowed the instrument to automatically adjust its settings for 25 °C.

## Drug Loading (DL) and Entrapment Efficiency (EE) Measurements

Drug entrapment efficiency (%EE) refers to the amount of drug that is successfully encapsulated within the nanoparticles, while drug loading refers to the ratio of the amount of drug encapsulated to the total weight of nanoparticles. These factors directly impact the efficiency and dosage accuracy of delivering drugs to target sites in the body. To measure the %EE and %DL of IVO in IVO-PLGA-NPs and IVO-CS-PLGA-NPs, colloidal solutions were centrifuged at 6000 rpm for 10 minutes to separate the supernatant and free drug in supernatant was analyzed by UV-Vis spectrophotometer at 284 nm. The equations 1 and 2, respectively, were used to calculate the %EE and %DL.

$$\% EE = \frac{\text{weight of IVO in NPs}}{\text{total weight of IVO used in NPs preparation}} \times 100 \quad (1)$$

$$\% DL = \frac{\text{weight of IVO in NPs}}{\text{weight of NPs}} \times 100 \quad (2)$$

## DSC Studies

DSC (Differential Scanning Calorimetry) has emerged as a valuable tool for evaluating the encapsulation of drugs in polymers. This technique allows to gain insight into the thermal behavior and interactions between the drug and polymer. DSC spectra of studies of free-IVO, blank-NPs, IVO-PLGA-NPs and IVO-CS-PLGA-NPs were recorded using DSC instrument “(Shimadzu DSC-60, Shimadzu Corporation, Tokyo, Japan)”. The samples under investigation (5 mg) were compressed in aluminium pan, kept in a sample holder against an empty reference pan and heated at a rate of 20° C per minute between 50°C and 250°C. The generated spectra were recorded and analyzed by software.

## Fourier Transforms Infra-Red (FTIR) Spectral Studies

The pure-IVO, blank-NPs, IVO-PLGA-NPs, and IVO-CS-PLGA-NPs FTIR spectra were taken using instrument “FTIR spectrometer (Jasco FTIR Spectrophotometer, Japan)”. The samples transparent pellets were prepared by KBr technique and FTIR spectra were recorded in the range of wavenumber 400–4000 cm<sup>-1</sup>.

## In-Vitro Release of IVO from Nanoparticles

The in-vitro drug release studies of nanoparticles were conducted using phosphate buffer (pH 6.8) 0.5% SLS as dissolution media. Accurately weighed amount of IVO-PLGA-NPs and IVO-CS-PLGA-NPs (equivalent to 5 mg of IVO) were suspended in PB (25 mL). After that, the solution was divided into several centrifuge tubes and maintained at 37 °C with 100 rpm of agitation on a biological shaker.<sup>24</sup> At every time interval, a centrifuge tube was taken out and centrifuged for 5 minutes at 6000 rpm. The supernatant was then examined for drug release using a UV/Vis spectrophotometer set to 284 nm.

Furthermore, release data of IVO-CS-PLGA-NPs were fitted using a variety of kinetic models, including the zero-order, first-order, Higuchi, and Korsmeyer-Peppas models, in order to obtain a better understanding of the drug release process.<sup>25,26</sup> These models served as valuable tools in analyzing and predicting the release mechanism of the drug over time. To select the most appropriate model for the drug release, careful consideration was given to the coefficient of correlation ( $R^2$ ) values obtained from each model. The model with the highest  $R^2$  value was chosen, indicating its superior fit to the release data.

## Storage Stability Studies

The storage stability tests at different temperatures play a crucial role in understanding the behavior of nanoparticles over time. For three months, the lyophilized IVO-PLGA-NPs and IVO-CS-PLGA-NPs powders were kept at 25 °C and 37 °C in an amber-colored vial. Samples were taken every 0, 30, 60 and 90 days, and their size, PDI, and ZP were examined.<sup>27</sup>

## In-Vitro Cytotoxicity Studies

### HepG2 Cells Growth and Maintenance

The HepG2 cells were procured from the American Type Culture Collection (Manassas, VA, USA). “Dulbecco’s Modified Eagle Medium (DMEM) (UFC Biotech, Riyadh, KSA)” was used to cultivate cells in 50 cm<sup>2</sup> tissue culture flasks at 37 °C in an incubator with 5% CO<sub>2</sub> humidity. The supplementation of the media included 10% fetal bovine serum ‘(Alpha Chemika, Mumbai, India)’, 1% of a combination of Penicillin (100 units/mL) and Streptomycin (100 µg/mL) from ‘ThermoFischer Scientific, Massachusetts, USA’, Amphotericin-B (250 ng/mL) from Gibco® (New York, USA), and 1% of L-glutamine ‘(BioWest, MO, USA)’. The MTT was bought from ‘Sigma in Aldrich, Missouri, in the United States’. DMEM was used to seed the cells in the culture plates.

### MTT Assay Against HepG2 Cell Lines

IVO has emerged as a highly effective treatment option for leukemia and bile duct cancers. Its remarkable potential in targeting and inhibiting specific mutations has revolutionized the field of cancer treatment. In the present research work, repurposing IVO for liver cancer intervention was investigated to decipher its therapeutic prospect, which has not been explored to date. The MTT assay was performed on HepG2 liver cells lines to determine whether IVO-PLGA-NPs and IVO-CS-PLGA-NPs have any potential anticancer effects in comparison to free-IVO and blank-NPs. Therefore, the MTT assay was performed on HepG2 cells to check the potential anticancer efficacy of the free-IVO, IVO-PLGA-NPs and IVO-CS-PLGA-NPs as compared to the free-IVO and blank-NPs. The MTT assay was used to determine the viability of the treated cells in order to evaluate the anticancer activity of free-IVO, IVO-PLGA-NPs, and IVO-CS-PLGA-NPs against HepG2 cells. This assay’s primary technique for determining the quantity of viable cells is mitochondria-mediated apoptosis. This section’s assay involves enzymatic reduction of 3-(4, 5-dimethylthiazol-2-yl)-2, 5-diphenyltetrazolium bromide (MTT), a water-soluble dye. This reduction process leads to the formation of an insoluble formazan compound. The quantitation of formazan is used as a measure of cell viability.<sup>28,29</sup> In this particular case, the cells were carefully seeded in a 96-well microplate with 100 µL of medium. This allows for optimal growth conditions and facilitates the subsequent steps of the assay. The suspension of free-IVO, IVO-PLGA-NPs, and IVO-CS-PLGA-NPs, with an IVO concentration ranging from 0.39 to 200 µg/mL were prepared using media as a diluents.<sup>30</sup> After the medium was removed, the cells were exposed to IVO-PLGA-NPs and IVO-CS-PLGA-NPs for 48 hours. The cells in the control group were only exposed to the medium. The drug-exposed cells were then given 100 µL of MTT solution (5 mg/mL) in PBS after a 48-hour period. After treating the cells with 20 µL of MTT, the grown cells were again incubated for four hours at 37 °C, but their media was replaced with new media without any drug. The subculture fluids were then discarded, and the MTT crystals were dissolved in a mixture of DMSO, acetic acid, and sodium dodecyl sulfate (99.4 mL, 0.6 mL, and 10 g) for 15 minutes at room temperature. Optical density (OD) was determined using a spectrophotometric microplate reader “(Synergy HT, BioTek gadgets, VT, USA)” at 570 nm. Using Eq. 3, the cell viability (%) was determined. The results were plotted as cell viability (%) versus log concentration of IVO (µg/mL) and normalized relative to that obtained for viable control cells, which were regarded as 100%. Using GraphPad Prism V-5.1, the IC<sub>50</sub> values were computed as log (inhibitor) versus normalized response on variable slopes.

$$\text{Cell Viability (\%)} = \frac{(\text{OD of test samples} - \text{OD of blank})}{(\text{OD of control} - \text{OD of blank})} \times 100 \quad (3)$$

### Activities of p53, Caspase-3, and Caspase-9 by ELISA

The p53, Caspase-3, and Caspase-9 activities were measured using ELISA kits in compliance with published works and manufacturer's instructions.<sup>31,32</sup> In 96-well plates, 5×10<sup>4</sup> HepG2 cells per well were seeded. The seeded cells had been dealt with the AqS of pure-IVO, IVO-PLGA-NPs and IVO-CS-PLGA-NPs. The concentration of IVO was kept 20 µg/mL, which was approximately near to the IC<sub>50</sub> value of the pure IVO (19.74 µg/mL) ie 1 × IC<sub>50</sub> of pure drug. The control group consisted of the untreated cells. After allowing each treated cell to come to room temperature, 100 µL of the p<sup>53</sup>, Caspase-3, and Caspase-9 reagents were added to each well in the plate that held 100 µL of culture media. The plates were correctly covered, agitated at 500 rpm for one to two minutes, and then allowed to incubate at room temperature. After an hour of incubation, the optical density (OD) was determined using a microplate reader at a wavelength of 405 nm.

### Evaluation of Morphological Changes in HepG2 Treated Cells

Morphological studies play a vital role in understanding the physical structure and characteristics of biological cells. In particular, phase contrast microscopy has emerged as a valuable tool for observing cellular morphology. To initiate the study, HepG2 cells were carefully seeded in 6-well plates at a density of 1×10<sup>5</sup> cells per well containing DMEM “(Dulbecco's Modified Eagle Medium)” and were incubated for 24 hours at 37 °C in 5% CO<sub>2</sub>. Thereafter, HepG2 cells were treated with the control, free-IVO, blank PLGA-NPs, IVO-PLGA-NPs and IVO-CS-PLGA-NPs, and were incubated for 24 hours. After that, cells were examined for alterations in cell structure or apoptosis using phase contrast microscopes “(Olympus CLX 41, Olympus Corporation, Tokyo, Japan)”, and images were recorded.

### Statistical Data Evaluation

All data were provided as mean ± standard deviation (SD). Statistical significance was determined using one-way analysis of variance (ANOVA) followed by a Bonferroni's multiple comparison test, depending on the number of groups being compared. The level of significance was set at P < 0.05.

## Results and Discussion

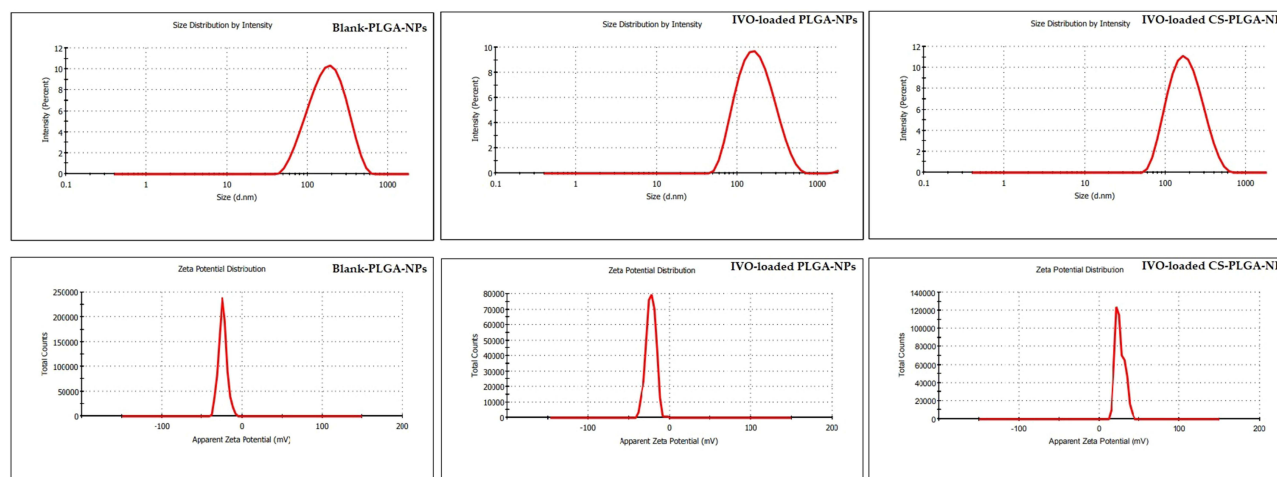
### Mean Particle Size, Polydispersity Index (PDI) and Zeta Potential

Table 2 lists the size, PDI, and ZP of the developed NPs. The size of the particles has a significant impact on how anti-cancer medications target tumors through circulation, biodistribution, accumulation, and penetration mechanisms.<sup>33</sup> The mean diameter of blank PLGA-NPs, IVO-loaded PLGA NPs and IVO-loaded CS-PLGA NPs was measured as 169.8 nm, 171.7 nm and 177.3 nm, respectively. However, the particle size of IVO-loaded CS-PLGA NPs increased from 171.7 nm to 177.3 nm upon chitosan coating, as measured by DLS method (Figure 1). Improved permeability and retention (EPR) effect-based accumulation in mature solid tumors has been shown to be best achieved with the use of nanoparticles whose average sizes fall between 100 and 400 nm.<sup>34</sup> The values obtained for the PDI of the prepared NPs, ranging from 0.304 to 0.333, provide clear evidence of the formation of monodispersed nanoparticles, size distribution of the particles is relatively narrow and uniform, with minimal variation in particle size. ZP refers to the surface charge that exists on nanoparticles, which influences their stability and interactions with other particles or surfaces. ZP values for blank-PLGA

**Table 2** Characterization of Nanoparticles

Formulations	Particle Size (nm)	PDI	ZP (mV)	%EE	%DL
Blank-PLGA-NPs	169.8±6.2	0.304±0.001	-24.0±5.2	-	-
IVO-PLGA-NPs	171.7±4.9	0.333±0.002	-23.0±5.8	96.3±4.3	9.66±1.1
IVO-CS-PLGA-NPs	177.3±5.2	0.311±0.002	+25.9±5.7	90.8±5.7	9.42±0.7





**Figure 1** Dynamic Scattering Light (DLS) particle size and zeta potential measurements of Blank-PLGA-NPs, IVO-PLGA-NPs and IVO-CS-PLGA-NPs.

-NPs and IVO-loaded PLGA NPs were  $-24.0$  mV and  $-23.0$  mV, respectively. The negative values are caused by the presence of a carboxylic group on the PLGA polymer's surface.<sup>16</sup> Post coating with chitosan, ZP of IVO-loaded CS-PLGA NPs was shifted to positive value,  $+25.9$  mV, due to protonation of nanoparticle surface. The electrostatic stability of colloidal suspensions can be predicted and regulated using the zeta potential, which is a crucial surface charge indicator. Coating with CS polymer caused the zeta potential to rise to a constant level. Because of its polycationic properties of CS, It is bioadhesive and water soluble, easily adhering to negatively charged surfaces of mucosal membranes. Consequently, it strengthens the mucosa's adherence, lengthening the time of contact for penetration of drug molecule through it.<sup>35,36</sup>

## Drug Loading (DL) and Entrapment Efficiency (EE) Measurements

The encapsulation of drugs within a polymeric matrix hinges on the crucial factors of affinities and compatibility. When a drug exhibits higher compatibility and affinity for the polymers, its encapsulation efficiency is significantly enhanced. The %EE and %DL of IVO in IVO-PLGA-NPs were measured as  $96.3 \pm 4.3\%$  and  $9.66 \pm 1.1\%$ , respectively. However, % EE and %DL of IVO in IVO-CS-PLGA-NPs were found as  $90.8 \pm 5.7\%$  and  $9.42 \pm 0.7\%$ , respectively (Table 2).

## DSC Studies

A comparative DSC spectra of free-IVO, blank-NPs, IVO-PLGA-NPs and IVO-CS-PLGA-NPs are shown in Figure 2. A sharp endothermic peak of free-IVO could be seen at the temperature  $157^\circ\text{C}$ , which is characteristics of pure drug.<sup>37</sup> However, the absence of IVO peak in the DSC curve of IVO-loaded nanoparticles represented that the drug in the nanoparticles was converted to amorphous phase during nanoparticle preparation. In other words, encapsulation process disrupted the IVO crystals, indicating that the encapsulation process was appreciable.<sup>38</sup> The broad endothermic peak could be seen in DSC spectra of IVO-PLGA-NPs and IVO-CS-PLGA-NPs, probably due to the presence of polymers or surfactants.

## FTIR Studies

The FTIR spectra of pure-IVO, IVO-PLGA-NPs and IVO-CS-PLGA-NPs are depicted in Figure 3. The pure-IVO demonstrated with typical characteristic peaks at  $3205\text{ cm}^{-1}$  (-NH- str),  $3072\text{ cm}^{-1}$  (-CH- str),  $2239\text{ cm}^{-1}$  (-C $\equiv$ N str),  $1730\text{ cm}^{-1}$  (-C=O- str),  $1651\text{ cm}^{-1}$  (-C=C- str),  $889\text{ cm}^{-1}$  (-CF<sub>2</sub>- str) and  $703\text{ cm}^{-1}$  (-CCl- str). The results showed an interesting trend in the absorption peaks observed in the fingerprint region ( $1600\text{--}400\text{ cm}^{-1}$ ). In both FTIR spectra of IVO-PLGA-NPs, and IVO-CS-PLGA-NPs, these peaks either disappeared or weakened significantly compared to pure-IVO. FTIR spectra of blank-NPs clearly evidenced non-overlapping of IVO peaks in drug loaded nanoparticles. This suggests that there was a successful entrapment of the drug inside the polymeric matrix. This finding highlights the

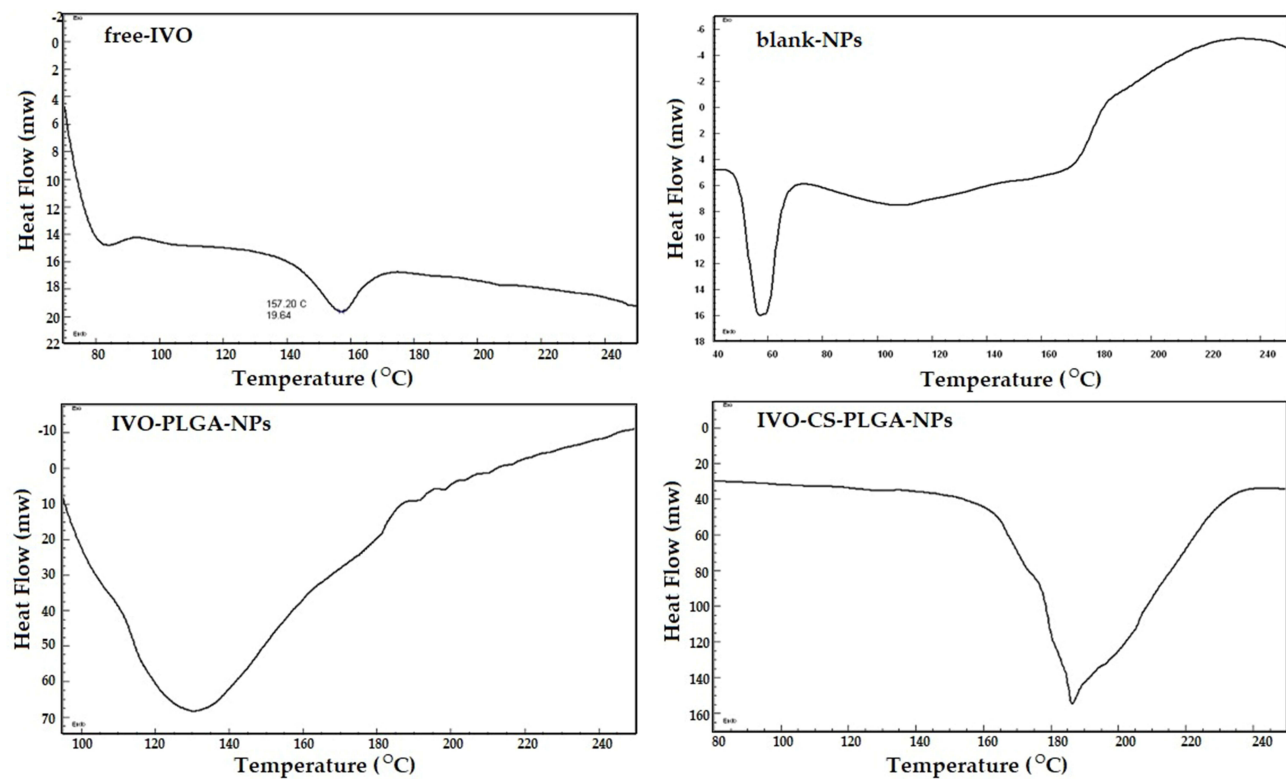


**Figure 2** DSC spectra of pure-IVO and their nanoparticles.

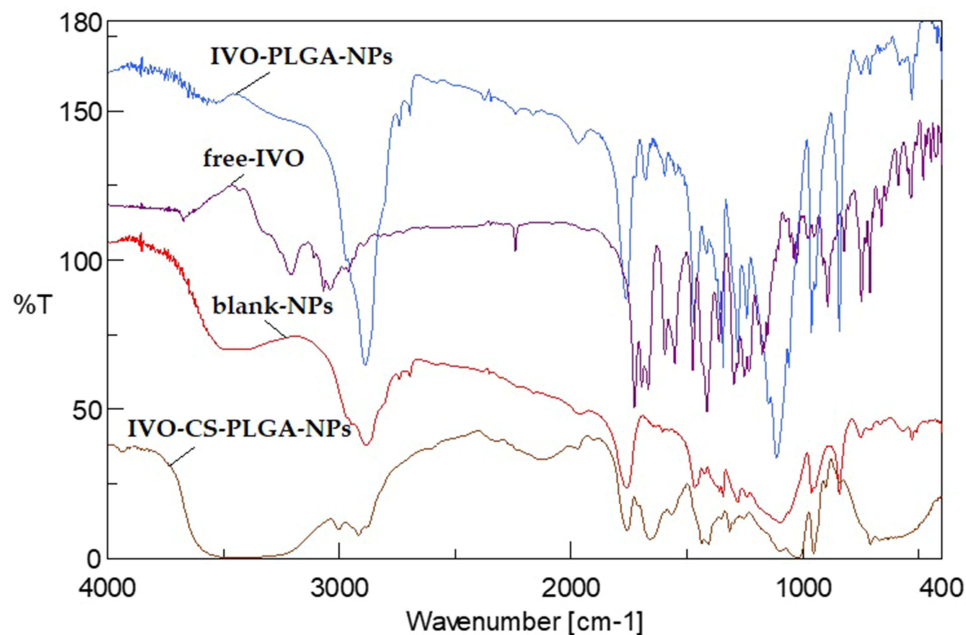


**Figure 3** FTIR spectra of pure-IVO and nanoparticles.

efficient encapsulation capability of both PLGA-NPs and chitosan-coated PLGA nanoparticles. The disappearance or weakening of absorption peaks indicates that the drug molecules were effectively incorporated within the polymeric structure, preventing their direct interaction with infrared radiation during FTIR analysis.

## In-Vitro Release of IVO from Nanoparticles

The in vitro release studies of IVO from IVO-PLGA-NPs and IVO-CS-PLGA-NPs were performed at pH 6.8 containing 0.5% w/v SLS and compared with free-IVO (Figure 4). A biphasic pattern was observed, consisting of a rapid drug release phase during the first five hours, succeeded by a gradual release phase lasting for the remaining 72 hours. For IVO-PLGA-NPs and IVO-CS-PLGA-NPs, the magnitude of the burst release in the first four hours was approximately 46.53% and 38.77%, respectively. The initial burst release of the drug could have been caused by the drug being adsorbed on the surface of excess IVO-containing nanoparticles that quickly dissolved into the media from the matrix.<sup>39,40</sup> The IVO-PLGA-NPs and IVO-CS-PLGA-NPs released 98.73% and 92.06±2.06% in 72 hours, respectively. The IVO-PLGA-NPs demonstrated complete release by the 72 hour, suggesting an effective sustained release.<sup>41</sup> Chitosan-coated PLGA NPs (IVO-CS-PLGA-NPs) indicated a controlled and sustained release, slightly slower than IVO-PLGA-NPs, this could be due to the chitosan which get swelled by time and retards the drug diffusion. The release profile data of IVO-CS-PLGA-NPs were fitted to the zero, first orders, Higuchi and Korsmeyer-Peppas models in order to find out the release mechanism, best fit was selected based on the  $R^2$  values of each drug release kinetics. The calculated  $R^2$  of zero, first, Higuchi and Korsmeyer-Peppas models were found as 0.7141, 0.8783, 0.8061, and 0.9723, respectively. The release behavior, suggesting a potential dominance of this Korsmeyer-Peppas model in postulating the IVO release. The “n” value of 0.312 further supports the Korsmeyer-Peppas model, indicating a release mechanism involving both diffusion and polymer relaxation, aligning with anomalous transport characteristics. The low “n” value (0.312) of IVO-CS-PLGA-NPs aligns with a non-Fickian diffusion or anomalous transport, where both diffusion and polymer relaxation significantly contribute to IVO release.

## Storage Stability Studies

After being stored at  $25 \pm 1^\circ\text{C}$  and  $37 \pm 1^\circ\text{C}$  for a period of time, the IVO-PLGA-NPs and IVO-CS-PLGA-NPs were examined for particle size, PDI, and ZP at various intervals (0, 30, 60 and 90 days). Table 3 presents the tabulated results. At either storage temperature, no significant changes were found in the particle size, PDI, and ZP. Therefore, without appreciably losing their physical properties, the developed nanoparticles can be stored at  $25 \pm 1^\circ\text{C}$  and  $37 \pm 1^\circ\text{C}$  for up to three months.

## MTT Assay Against HepG2 Cell Lines

The cytotoxicity potential of pure-IVO, IVO-loaded PLGA and IVO-loaded CS-coated PLGA NPs against HepG2 cells (percent cell viability at different concentrations), as well as log drug concentration vs percent cell viability were depicted

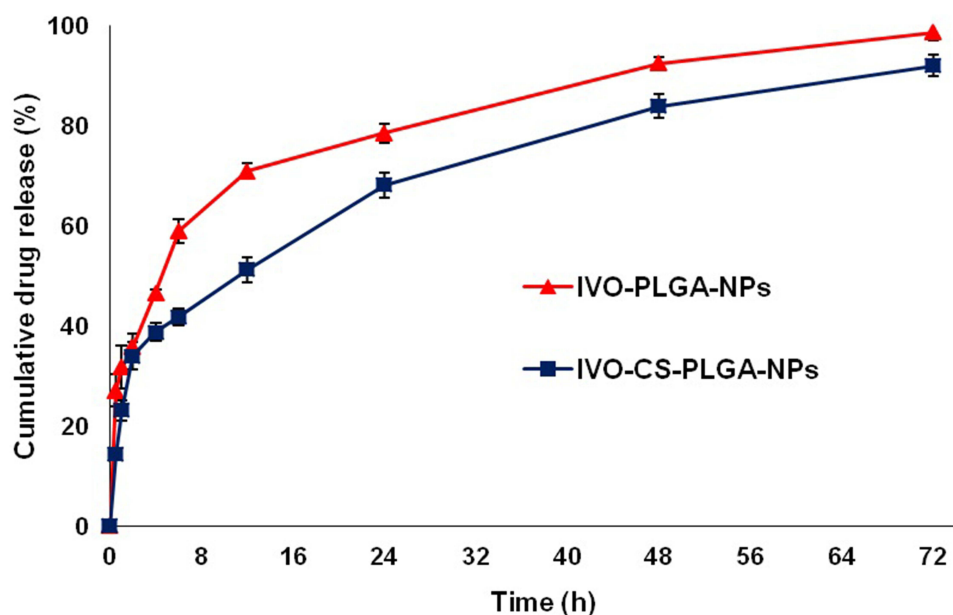


**Figure 4** In-vitro release profile of IVO from IVO-PLGA-NPs and IVO-CS-PLGA-NPs at pH 6.8.



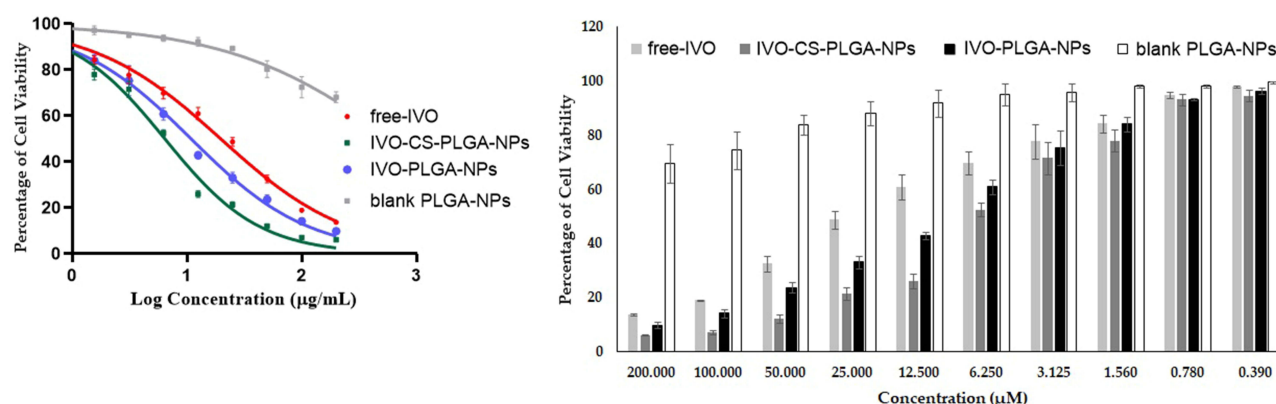
**Table 3** Particle Characterization of After Storage at Different Temperature (25 °C & 37 °C)

Time (days)	Conditions	IVO-PLGA-NPs			IVO-CS-PLGA-NPs		
		Size (nm)	PDI	ZP (mV)	Size (nm)	PDI	ZP (mV)
0	-	171.7±4.9	0.333±0.002	-23.0±5.8	177.3±5.2	0.311±0.002	+25.9±5.7
30	25 °C	179.3±5.0	0.338±0.001	-22.5±4.5	184.5±4.7	0.318±0.001	+25.5±2.5
60		184.2±5.2	0.339±0.002	-21.7±3.1	189.3±6.3	0.323±0.002	+24.8±2.8
90		194.6±3.8	0.373±0.013	-19.8±1.8	199.4±4.3	0.336±0.011	+24.7±2.4
30	37 °C	179.7±5.1	0.383±0.011	-22.1±3.3	179.5±4.0	0.325±0.012	+25.2±1.9
60		187.3±7.2	0.410±0.016	-20.4±3.5	188.4±6.6	0.338±0.010	+24.1±3.6
90		201.3±6.1	0.413±0.015	-17.2±3.2	200.9±7.4	0.431±0.002	+23.8±4.4

in Figure 5. The concentration-dependent decrease in percent cell viability was confirmed by the IVO concentrations. The IC<sub>50</sub> values of pure-IVO, IVO-loaded PLGA NPs and IVO-loaded CS-coated PLGA NPs against HepG2 cells were 19.74 µg/mL ( $R^2 = 0.9841$ ), 10.90 µg/mL ( $R^2 = 0.9908$ ) and 6.43 µg/mL ( $R^2 = 0.9855$ ), respectively. The data of MTT assay against HepG2 cells in the present investigation, revealed a significant ( $p < 0.05$ ) enhancement in the cytotoxic effect of IVO-loaded PLGA NPs and IVO-loaded CS-coated PLGA NPs in comparison to pure-IVO. The enhanced cytotoxicity of IVO-loaded PLGA NPs and IVO-loaded CS-coated PLGA NPs relative to free-IVO could be attributed to the carrier's nanoscale size, enhanced encapsulation and cellular uptake. Therefore, developed IVO-loaded PLGA NPs and IVO-loaded CS-coated PLGA NPs could be a potential alternative to the conventional formulation of IVO against liver cancer.

### p<sup>53</sup>, Caspase-3 and Caspase-9 Activities by ELISA

Understanding the activities of these key players, such as p53 (a tumor suppressor protein), along with caspase-3 and -9, is vital for comprehending the intricate mechanisms underlying cellular apoptosis. By studying their activities, it can gain valuable insights into diseases related to aberrant cell death regulation like cancer and neurodegenerative disorders.<sup>42</sup> In the present investigation, an intriguing finding was observed regarding the expression of the p<sup>53</sup> protein. The study revealed a significant increase ( $p < 0.05$ ) in p<sup>53</sup> expression in the free-IVO, IVO-PLGA-NPs and IVO-CS-PLGA-NPs groups, compared to the control (untreated group) (Table 4). The p53 expression were 3.79, 4.26 and 4.56 folds higher when the cells were treated with free-IVO, IVO-PLGA-NPs and IVO-CS-PLGA-NPs groups, compared to the control (untreated group). This notable increase suggests a highly efficient apoptotic activity of IVO-CS-PLGA-NPs > free-IVO

**Figure 5** Cell viability tests and IC<sub>50</sub> values after 48 hours of pure-IVO, IVO-loaded PLGA and IVO-loaded CS-coated PLGA NPs against HepG2 cells.

**Table 4** Activities of p53, Caspase-3 and Caspase-9 of HepG2 Treated Cells

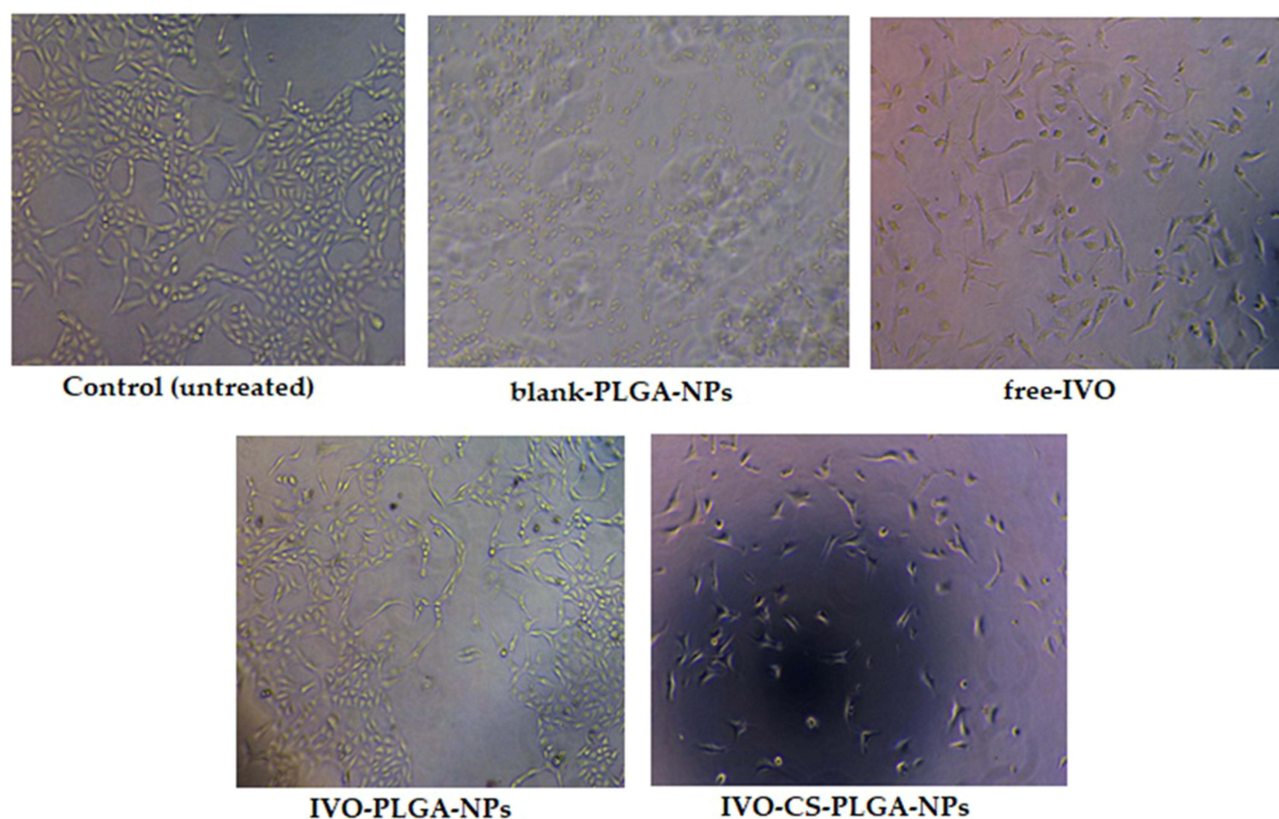
Codes	P53		Caspase 3		Caspase 9	
	Conc (pg/mL)	Fold Change	Conc (pg/mL)	Fold Change	Conc (pg/mL)	Fold Change
Control (Untreated)	285.67±49.28	1.00±0.17	46.31±10.22	1.00±0.22	8.47±0.42	1.00±0.05
Blank PLGA-NPs	334.00±49.00	1.17±0.17	69.91±15.33	1.51±0.33	9.37±0.38	1.11±0.05
Free-IVO	1084.00±74.93	3.79±0.26	128.91±20.44	2.78±0.44	11.98±0.61	1.41±0.07
IVO-PLGA-NPs	1217.33±101.52	4.26±0.36	190.86±13.52	4.12±0.29	12.16±0.27	1.44±0.31
IVO-CS-PLGA-NPs	1302.33±69.12	4.56±0.24	285.25±22.27	6.16±0.48	16.22±0.82	1.91±0.09

against HepG2 cells. The upregulation of p<sup>53</sup> protein expressions further supports the effectiveness of these treatments in inducing programmed cell death in cancer cells. The expression levels of Caspase-3 and Caspase-9 in IVO-PLGA-NPs and IVO-CS-PLGA-NPs treated groups (Table 1) showed a noteworthy increase compared to the untreated control group.

When the HepG2 cells were treated with IVO-PLGA-NPs and IVO-CS-PLGA-NPs, approximately 4.1-folds and 6.1-folds increased activities of Caspase-3; 1.4-folds and 1.9-folds increased expression of Caspase-9, respectively, were noted as compared to the untreated (control) cells. The elevated expression levels of Caspase-3 and Caspase-9 indicate that both IVO-PLGA-NPs and IVO-CS-PLGA-NPs have significant apoptotic activities in HepG2 cells.

## Evaluation of Morphological Changes in HepG2 Treated Cells

Figure 6 depicts the morphological changes of HepG2 cells after treatment control, free-IVO, blank PLGA-NPs, IVO-PLGA-NPs and IVO-CS-PLGA-NPs. Moderate decrease in HepG2 cell numbers was observed following treatment with

**Figure 6** Morphological changes of HepG2 cells after treatment with control, free-IVO, blank PLGA-NPs, IVO-PLGA-NPs.

IVO-PLGA-NPs and IVO-CS-PLGA-NPs compared to the blank PLGA-NPs and control. The HepG2 cells treated with IVO-PLGA-NPs and IVO-CS-PLGA-NPs exhibited shrinkage and reduction in adherent viable cells and an increase in floating dead cells, shapes also change to irregular and most of them are dead.<sup>43</sup> The MTT assay data are consistent with these results.

## Conclusion

We successfully developed and evaluated IVO-loaded-PLGA-NPs and IVO-loaded-CS-PLGA-NPs. The prepared nanoparticles exhibited an acceptable particle, PDI, zeta potential, high drug encapsulation and sustained drug release. The enhanced cytotoxicity and lower IC<sub>50</sub> values for IVO-loaded-PLGA-NPs and IVO-loaded-CS-PLGA-NPs indicate that they outperform free IVO. Compared to free-IVO and blank-PLGA-NPs, the IVO-loaded-PLGA-NPs and IVO-loaded-CS-PLGA-NPs showed higher cytotoxic, p53, caspase-3 and caspase-9 activities against HepG2 cell lines. The chitosan coated nanoparticles (IVO-CS-PLGA-NPs) exhibited superior efficacy than IVO-PLGA-NPs. Based on the promising findings, it is suggested that repurposing ivosidenib and encapsulating it into chitosan-coated PLGA-NPs could be a compelling approach to effectively treat liver cancer. These chitosan-coated PLGA-NPs can be given by oral route. This will further reduce the toxic effects associated with IVO by decreasing the frequency and reducing the dose.

## Acknowledgments

The authors extend their appreciation to the Deputyship for Research & Innovation, Ministry of Education in Saudi Arabia for funding this research through the project number (IF2/PSAU-2022/03/22082).

## Funding

The authors extend their appreciation to the Deputyship for Research & Innovation, Ministry of Education in Saudi Arabia for funding this research through the project number (IF2/PSAU-2022/03/22082).

## Disclosure

The authors report no conflicts of interest in this work.

## References

1. Man S, Luo C, Yan M, Zhao G, Ma L, Gao W. Treatment for liver cancer: from sorafenib to natural products. *Eur J Med Chem*. 2021;224:113690. doi:10.1016/j.ejmech.2021.113690
2. Calderaro J, Ziol M, Paradis V, Zucman-Rossi J. Molecular and histological correlations in liver cancer. *J Hepatol*. 2019;71(3):616–630. doi:10.1016/j.jhep.2019.06.001
3. Sell S, Leffert HL. Liver cancer stem cells. *J Clin Oncol*. 2008;26(17):2800–2805. doi:10.1200/JCO.2007.15.5945
4. Dhillon S. Ivosidenib: first global approval. *Drugs*. 2018;78(14):1509–1516. doi:10.1007/s40265-018-0978-3
5. Norsworthy KJ, Luo L, Hsu V, et al. FDA approval summary: ivosidenib for relapsed or refractory acute myeloid leukemia with an isocitrate Dehydrogenase-1 mutation. *Clin Cancer Res*. 2019;25(11):3205–3209. doi:10.1158/1078-0432.CCR-18-3749
6. Casak SJ, Pradhan S, Fashoyin-Aje L, et al. FDA approval summary: ivosidenib for the treatment of patients with advanced unresectable or metastatic, chemotherapy refractory cholangiocarcinoma with an IDH1 mutation. *Clin Cancer Res*. 2022;28(13):2733–2737. doi:10.1158/1078-0432.CCR-21-4462
7. Center for drug evaluation and research application number 211192Orig1s000 multi-discipline review. Available from: [https://www.accessdata.fda.gov/drugsatfda\\_docs/nda/2018/211192Orig1s000MultidisciplineR.pdf](https://www.accessdata.fda.gov/drugsatfda_docs/nda/2018/211192Orig1s000MultidisciplineR.pdf). Accessed December 17, 2018.
8. Bhalani DV, Nutan B, Kumar A, Singh Chandel AK. Bioavailability enhancement techniques for poorly aqueous soluble drugs and therapeutics. *Biomedicines*. 2022;10(9):2055. doi:10.3390/biomedicines10092055
9. Kumari L, Choudhari Y, Patel P, et al. Advancement in solubilization approaches: a step towards bioavailability enhancement of poorly soluble drugs. *Life*. 2023;13(5):1099. doi:10.3390/life13051099
10. Tang X, Chen L, Li A, et al. Anti-GPC3 antibody-modified sorafenib-loaded nanoparticles significantly inhibited HepG2 hepatocellular carcinoma. *Drug Deliv*. 2018;25(1):1484–1494. doi:10.1080/10717544.2018.1477859
11. Dinarvand R, Sepehri N, Manoochehri S, Rouhani H, Atyabi F. Polylactide-co-glycolide nanoparticles for controlled delivery of anticancer agents. *Int J Nanomed*. 2011;6:877–895. doi:10.2147/IJN.S18905
12. Alvi M, Yaqoob A, Rehman K, et al. PLGA-based nanoparticles for the treatment of cancer: current strategies and perspectives. *AAPS Open*. 2022;8(1):12. doi:10.1186/s41120-022-00060-7
13. Makadia HK, Siegel SJ. Poly Lactic-co-Glycolic Acid (PLGA) as biodegradable controlled drug delivery carrier. *Polymers*. 2011;3(3):1377–1397. doi:10.3390/polym3031377

14. Gentile P, Chiono V, Carmagnola I, Hatton PV. An overview of poly(lactic-co-glycolic) acid (PLGA)-based biomaterials for bone tissue engineering. *Int J Mol Sci.* **2014**;15(3):3640–3659. doi:10.3390/ijms15033640
15. Kapoor DN, Bhatia A, Kaur R, et al. PLGA: a unique polymer for drug delivery. *Therap Deliv.* **2015**;6(1):41–58. doi:10.4155/tde.14.91
16. Alshetaili AS. Gefitinib loaded PLGA and chitosan coated PLGA nanoparticles with magnified cytotoxicity against A549 lung cancer cell lines. *Saudi J Biol Sci.* **2021**;28(9):5065–5073. doi:10.1016/j.sjbs.2021.05.025
17. Mikušová V, Mikuš P. Advances in chitosan-based nanoparticles for drug delivery. *Int J Mol Sci.* **2021**;22(17):9652. doi:10.3390/ijms22179652
18. Abd El Hady WE, Mohamed EA, Soliman OAE, El-Sabbagh HM. In vitro-in vivo evaluation of chitosan-PLGA nanoparticles for potentiated gastric retention and anti-ulcer activity of diosmin. *Int J Nanomed.* **2019**;14:7191–7213. doi:10.2147/IJN.S213836
19. Li T, Ashrafizadeh M, Shang Y, Nuri Ertas Y, Orive G. Chitosan-functionalized bioplatfroms and hydrogels in breast cancer: immunotherapy, phototherapy and clinical perspectives. *Drug Discov Today.* **2024**;29(1):103851. doi:10.1016/j.drudis.2023.103851
20. Ashrafizadeh M, Hushmandi K, Mirzaei S, et al. Chitosan-based nanoscale systems for doxorubicin delivery: exploring biomedical application in cancer therapy. *Bioeng Transl Med.* **2022**;8(1):e10325. doi:10.1002/btm2.10325
21. Ashrafizadeh M, Delfi M, Hashemi F, et al. Biomedical application of chitosan-based nanoscale delivery systems: potential usefulness in siRNA delivery for cancer therapy. *Carbohydr Polym.* **2021**;260:117809. doi:10.1016/j.carbpol.2021.117809
22. Anwer MK, Ali EA, Iqbal M, et al. Development of chitosan-coated PLGA-based nanoparticles for improved oral olaparib delivery: in vitro characterization, and in vivo pharmacokinetic studies. *Processes.* **2022**;10(7):1329. doi:10.3390/pr10071329
23. Ahmed MM, Anwer MK, Fatima F, et al. Boosting the anticancer activity of sunitinib malate in breast cancer through lipid polymer hybrid nanoparticles approach. *Polymers.* **2022**;14(12):2459. doi:10.3390/polym14122459
24. Fong SS, Foo YY, Saw WS, et al. Chi-tosan-coated-PLGA nanoparticles enhance the antitumor and antimigration activity of statin – a STAT3 dimerization blocker. *Int J Nanomed.* **2022**;17:137–150. doi:10.2147/IJN.S337093
25. Ritger PL, Peppas NA. A simple equation for description of solute release II. Fickian and anomalous release from swellable devices. *J Control Release.* **1987**;5(1):37–42. doi:10.1016/0168-3659(87)90035-6
26. Kalam MA, Iqbal M, Alshemery A, Alkholief M, Alshamsan A. Development and evaluation of chitosan nanoparticles for ocular delivery of tedizolid phosphate. *Molecules.* **2022**;27(7):2326. doi:10.3390/molecules27072326
27. Aljuffali IA, Anwer MK, Ahmed MM, et al. Development of gefitinib-loaded solid lipid nanoparticles for the treatment of breast cancer: physicochemical evaluation, stability, and anticancer activity in breast cancer (MCF-7) cells. *Pharmaceuticals.* **2023**;16(11):1549. doi:10.3390/ph16111549
28. Alshetaili AS, Ali R, Qamar W, et al. Preparation, optimization, and characterization of chrysin-loaded TPGS-b-PCL micelles and assessment of their cytotoxic potential in human liver cancer (Hep G2) cell lines. *Int J Biol Macromol.* **2023**;246:125679. doi:10.1016/j.ijbiomac.2023.125679
29. Ibrahim S, Baig B, Hisaindee S, et al. Development and evaluation of crocetin-functionalized pegylated magnetite nanoparticles for hepatocellular carcinoma. *Molecules.* **2023**;28(7):2882. doi:10.3390/molecules28072882
30. Fu L, Wang S, Wang X, et al. Crystal structure-based discovery of a novel synthesized PARP1 inhibitor (OL-1) with apoptosis-inducing mechanisms in triple-negative breast cancer. *Sci Rep.* **2016**;6(1):3. doi:10.1038/s41598-016-0007-2
31. Devarajan E, Sahin AA, Chen JS, et al. Down-regulation of caspase 3 in breast cancer: a possible mechanism for chemoresistance. *Oncogene.* **2002**;21(57):8843–8851. doi:10.1038/sj.onc.1206044
32. Md S, Alhakamy NA, Alharbi WS, et al. Development and evaluation of repurposed etoricoxib loaded nanoemulsion for improving anticancer activities against lung cancer cells. *Int J Mol Sci.* **2021**;22(24):13284. doi:10.3390/ijms222413284
33. Yu W, Liu R, Zhou Y, Gao H. Size-tunable strategies for a tumor targeted drug delivery system. *ACS Cent Sci.* **2020**;6(2):100–116. doi:10.1021/acscentsci.9b01139
34. Bawa R. Bio-nanotechnology: a revolution in food, biomedical and health science. Wiley-Blackwell; **2013**.
35. de Oliveira DG, Pimentel GA, Andrade GFS. Chitosan stabilization and control over hot spot formation of gold nanospheres and SERS performance evaluation. *Vib Spectrosc.* **2020**;110:103119. doi:10.1016/j.vibspec.2020.103119
36. Phan TTV, Phan DT, Cao XT, et al. Roles of chitosan in green synthesis of metal nanoparticles for biomedical applications. *Nanomaterials.* **2021**;11(2):273. doi:10.3390/nano11020273
37. Gu C-H, Sizemore JP, Zhang S. Ivosidenib forms and pharmaceutical compositions. US patent No. WO2020010058A1; **2020**.
38. Amjadi I, Rabiee M, Hosseini MS. Anticancer activity of nanoparticles based on PLGA and its co-polymer: in-vitro evaluation. *Iran J Pharm Res.* **2013**;12(4):623–634.
39. Lemoine D, Francois C, Kedzierewicz F, et al. Stability study of nanoparticles of poly ( $\epsilon$ -caprolactone), poly (D,L-lactide) and poly(D,L-lactide-co-glycolide). *Biomaterials.* **1996**;17(22):2191–2197. doi:10.1016/0142-9612(96)00049-X
40. Lamprecht A, Ubrich N, Perez H, et al. Influences of process parameters on nanoparticle preparation performed by a double emulsion pressure homogenization technique. *Int J Pharm.* **2000**;196(2):177–182. doi:10.1016/S0378-5173(99)00422-6
41. Malhotra M, Majumdar DK. Permeation through cornea. *Indian J Exp Biol.* **2001**;39:11–24.
42. Jan R, Chaudhry GE. Understanding apoptosis and apoptotic pathways targeted cancer therapeutics. *Adv Pharm Bull.* **2019**;9(2):205–218. doi:10.15171/apb.2019.024
43. Sun SJ, Deng P, Peng CE, et al. Selenium-modified chitosan induces HepG2 cell apoptosis and differential protein analysis. *Cancer Manag Res.* **2022**;14:3335–3345. doi:10.2147/CMAR.S382546

## International Journal of Nanomedicine

Dovepress

**Publish your work in this journal**

The International Journal of Nanomedicine is an international, peer-reviewed journal focusing on the application of nanotechnology in diagnostics, therapeutics, and drug delivery systems throughout the biomedical field. This journal is indexed on PubMed Central, MedLine, CAS, SciSearch®, Current Contents®/Clinical Medicine, Journal Citation Reports/Science Edition, EMBase, Scopus and the Elsevier Bibliographic databases. The manuscript management system is completely online and includes a very quick and fair peer-review system, which is all easy to use. Visit <http://www.dovepress.com/testimonials.php> to read real quotes from published authors.

Submit your manuscript here: <https://www.dovepress.com/international-journal-of-nanomedicine-journal>